Application of Stone-Derived Substrates in Thin-Film Temperature Sensing

Niloofar Saeedzadeh Khaanghah, *Member, IEEE*, Hugo de Souza Oliveira, *Member, IEEE*, Soufiane Krik, *Member, IEEE*, Alejandro Carrasco-Pena, *Member, IEEE*, Giuseppe Cantarella *Member, IEEE*, Michael Haller, *Member, IEEE*, Nicholas Rapagnani, Aart van Bezooijen, Michael Nippa, and Niko Münzenrieder, *Senior Member, IEEE*.

***Abstract*— Advancements in materials and technologies have enabled thin-film electronics to be directly developed on previously unsuitable substrates. This paper explores the fabrication of two thin-film temperature sensors, thermistors and resistance temperature detectors (RTD), using stone-based substrates, including marble, brick, stone paper, and Limex paper. The thermistors and RTDs were fabricated utilizing Cu / InGaZnO and Zn, applying the sputtering deposition technique. The sensor's performance was analyzed based on two different heating methodologies: one using a hotplate, and the other using a localized heating from above. The sensors' performance was characterized within a temperature range of $25\,^{\circ}\mathrm{C}$ to $80\,^{\circ}\mathrm{C}$. While the marble thermistor demonstrated the highest sensitivity among all thermistors at $-11.54\,\%\,^{\circ}\mathrm{C}^{-1}$, the stone paper RTD similarly showed the highest sensitivity among all RTDs at $0.77\,^{\circ}\mathrm{C}^{-1}$. The localized heating methodology on top of RTDs resulted in the stone paper and Limex showing negligible hysteresis. Moreover, the sensors demonstrated stable behavior in the multiple reliability tests. Furthermore, Zn-based RTDs were dissolvable in less than 36 hours. The outcomes show that stone-based materials are promising natural eco-friendly substrates for temperature sensors leading to less hazardous electronic waste.**

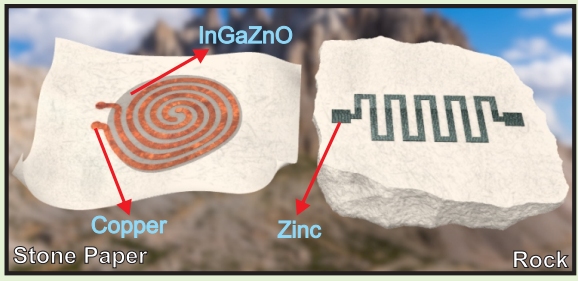

***Index Terms*— Thin-film sensors, Natural materials, Stone, Thermistor, RTD, InGaZnO**

I. Introduction

OVER the last few years, the advent of thin-film and flexible sensors [1] has enabled significant progress in the design and fabrication of innovative devices that show desirable attributes, such as bendability [2], stretchability [3], and conformability [4]. Hence, it opens up new frontiers in areas that were so far constrained by the traditional bulky electronics [5], such as novel interfaces [6], wearables [7], health monitoring [8], and machine learning data collecting [9]. These technological advancements have made it possible to have low-cost electronics integrated into our daily items. However, besides benefiting from these advantages, the environmental impact of massive electronics fabrication has turned out to be a significant concern.

Due to the use of non-recyclable materials and toxic elements, electronic waste (e-waste) is a growing problem. It poses a threat to the environment and human health particularly when it comes to wearable electronics. To address the e-waste problem, conventional recycling and reusing methods are not enough to eliminate the e-waste impacts. Therefore, further solutions are needed to be taken. While multifunctional sensors can bring cross-sensitivity to detect different parameters and reduce the number of individual sensors [10] [11], the use of biocompatible and biodegradable materials in sensor fabrication can be a practical approach. Traditionally, flexible thin-film sensors are fabricated using conventional plastic substrates, such as polyimide (PI) [12], polydimethylsiloxane (PDMS) [13], polymethyl methacrylate (PMMA) [14], and

Submitted for review xxxx 2024. 'This work is partially funded by the Autonomous Province of Bozen-Bolzano/South Tyrol through the International Joint-Project Cooperations South Tyrol-Switzerland (FLEXIBOTS, grant n.: 2/34), South Tyrol-Luxembourg (V-SAFE, grant n.: 7/34), as well as the Autonomous Province of Bozen-Bolzano/South Tyrol's European Regional Development Fund project: EFRE/FESR 1011-Smart Cover, and was partially carried out within the PNRR research activities of the consortium iNEST (Interconnected North-Est Innovation Ecosystem) funded by the European Union Next-GenerationEU (Piano Nazionale di Ripresa e Resilienza (PNRR) – Missione 4 Componente 2, Investimento 1.5 – D.D.1058 23/06/2022, ECS-00000043). This manuscript reflects only the Authors' views and opinions, neither the European Union nor the European Commission can be considered responsible for them.

Niloofar Saeedzadeh Khaanghah, Hugo de Souza Oliveira, Soufiane Krik, Alejandro Carrasco-Pena, Michael Haller, and Niko Münzenrieder are with the Faculty of Engineering, Free University of Bozen-Bolzano, Bozen-Bolzano, 39100, Italy (e-mail: niloofar.saeedzadehkhaanghah@student.unibz.it).

Giuseppe Cantarella is with the Department of Physics, Informatics and Mathematics, University of Modena and Reggio Emilia, Modena, 41125, Italy.

Nicholas Rapagnani, and Aart van Bezooijen are with the Faculty of Design and Art, Free University of Bozen-Bolzano, Bozen-Bolzano, 39100, Italy.

Michael Nippa is with the Faculty of Economics and Management, Free University of Bozen-Bolzano, Bozen-Bolzano, 39100, Italy.

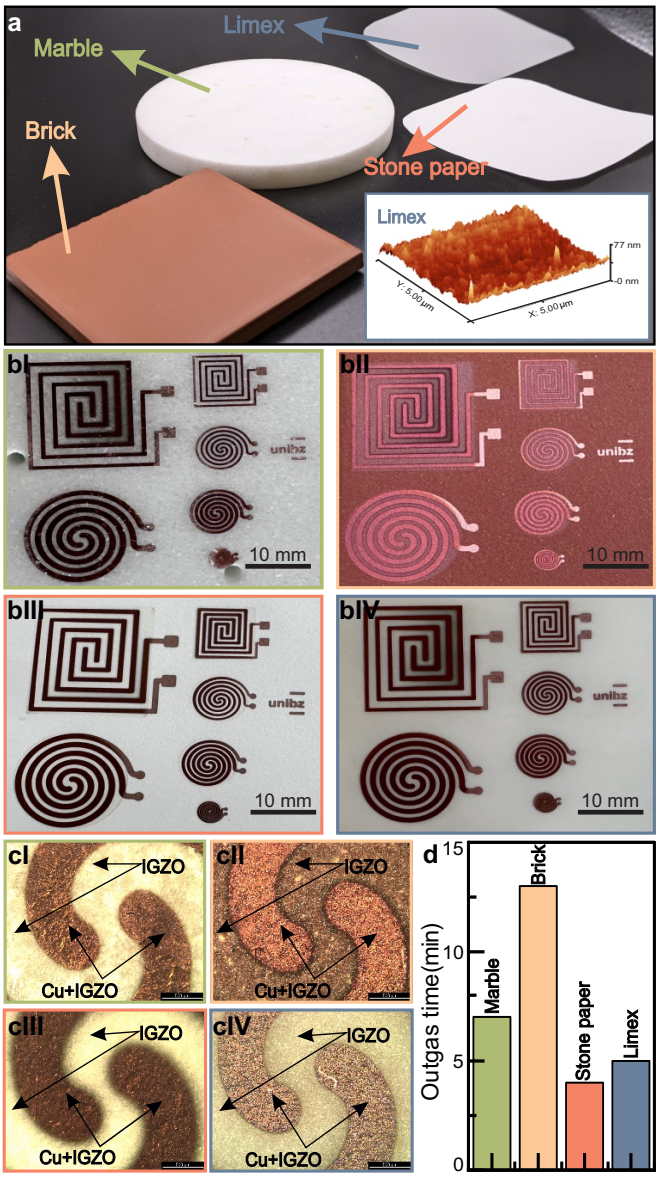

Fig. 1. Substrates and thermistors structures: a) Bare substrates [inset: AFM measurement of the Limex surface]; bI) Marble thermistor, bII) brick thermistor, bIII) stone paper thermistor, and bIV) Limex thermistor. c) Micrographs of a circular thermistor of (cI) marble thermistor, cII) brick thermistor, cIII) stone paper thermistor, and (cIV) Limex thermistor. d) Substrates outgas time inside the sputtering machine.

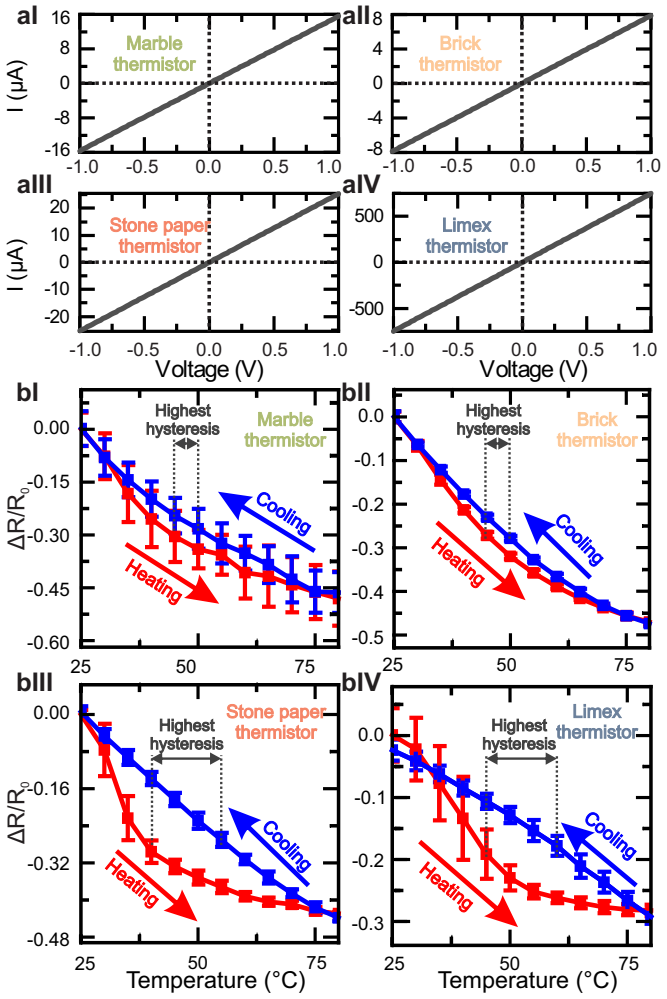

Fig. 2. Thermistors performances: Current-voltage characteristics of (aI) marble thermistor, aII) brick thermistor, aIII) stone paper thermistor, and (aIV) Limex thermistor. Normalized thermistors resistance versus temperature for (bI) marble thermistor, bII) brick thermistor, bIII) stone paper thermistor, and (bIV) Limex thermistor.

polyethylene terephthalate (PET) [10]. However, efforts have been made to minimize the environmental concerns of sensor fabrication waste by utilizing biodegradable and eco-friendly alternatives like cellulose-based materials and paper [15] [16].

Furthermore, there is great potential in exploring unconventional and novel substrates, which can either have the electronics directly fabricated onto them or receive it from a donor substrate through transferring techniques [17]. Besides offering important characteristics, such as recyclability [18] or biodegradability [19], stretchability [20], unconventional substrates can also bring functional properties like self-healability [3], and permeability [21], thereby enriching the application possibilities, as the sensor can be fabricated onto a wide range of materials, such as thin-foils and larger objects [22]. Such advancements not only broaden the potential uses of environmentally sustainable electronics and sensors but also pave the way for their integration into a wider array of everyday objects and devices that can be broken down into harmless or recyclable components.

Given the widespread measurement of temperature, there is a growing demand for highly sensitive temperature sensors that have a broad operating range, can conform to uneven surfaces in engineering, and safely interact with human skin. This has led researchers to explore various flexible materials for temperature sensing [23], [24]. Consequently, printing, coating, and deposition have become leading methods for flexible thin-film sensor fabrication [25]. Motivated by its roll-to-roll fabrication ease, availability, biodegradability, environmental friendliness, lightweight, and flexibility, the paper has attracted considerable interest as an electronic substrate, finding application in a diverse array of electronic devices including solar cells [26], organic LEDs (OLEDs) [27], biobatteries [28], sensors [29], transistors [30], displays [31], and radio frequency identification devices (RFID) [32].

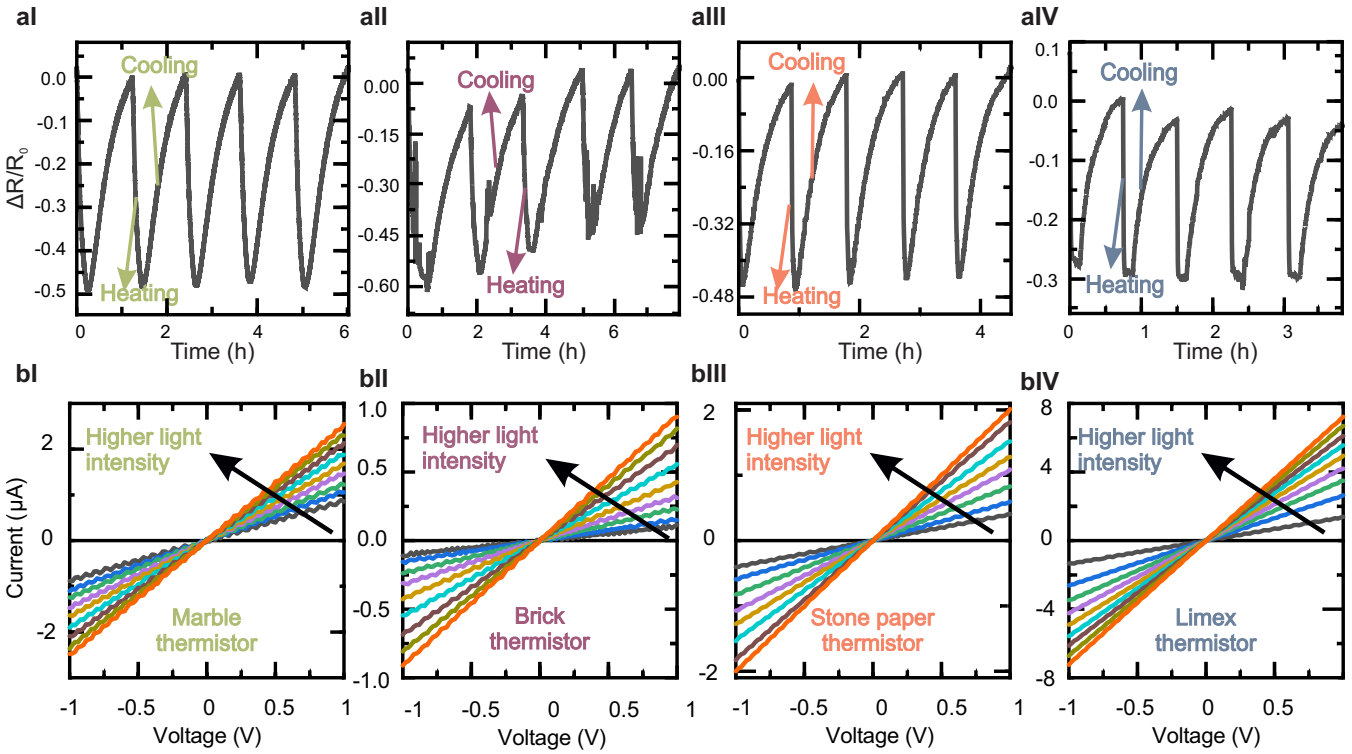

Fig. 3. Thermistors repeatability and light sensitivity: Cycling test and sensitivity of (a) Marble thermistor, b) Brick thermistor, c) Stone thermistor, and (d) Limex thermistor. b) Light sensitivity of (a) Marble thermistor, b) Brick thermistor, c) Stone thermistor, and (d) Limex thermistor.

Moreover, stone paper, also known as mineral paper, rock paper, or eco-paper, is similar to traditional cellulose paper in appearance. However, the stone paper, made of calcium carbonate obtained from industrial stone waste, is resistant to rips, water, and printing. Also, stone papers have a short lifespan when exposed to the environment [33]. Varodi et al. used stone paper to fabricate flexible screen-printed electrodes for electrochemical dopamine detection [34]. They used different types of paper as flexible substrates to fabricate lead sulfide (PbS) colloidal quantum dots photodetectors and noticed that stone paper worked the best for their device [35]. However, the potential of stone-based substrates in thin-film fabrication methods, particularly vacuum deposition methods, still requires comprehensive research.

This paper initially summarizes expansion information on manufacturing of amorphous InGaZnO (IGZO) based thermistors onto four unconventional environmentally friendly stone-based substrates that were previously published in the IEEE Sensors Conference [36]. The stone-based substrates consist of a raw stone, a heat-treated brick, and two commercial flexible substrates made from stone powder derived from calcium carbonate namely stone paper and Limex [37] [38]. As such these materials represent three different levels of processing. Subsequently, to advance the fabrication of entirely environmentally friendly temperature sensors on stone-based substrates, Zn-based RTDs were fabricated taking advantage of the biocompatibility and eco-friendliness of Zn. The findings indicate that stone paper and Limex can serve as viable alternatives to traditional "semi-natural" paper as offering treeless production, low carbon footprint, and full degradability [39]. Furthermore, using such unconventional substrates offers an alternative to conventional plastics for the fabrication of thin-film sensing devices, and reduces the use of single plastics which will rise from the demand for more Internet of Things (IoT) applications by converting the surfaces of objects functional and active, and in particular, also opens up ways to create sensors on aesthetically pleasing natural surfaces.

II. Materials and Methods

The thermistors are fabricated on natural stone and stone-based substrates. The substrates used in this work include marble with a thickness of $10\,\mathrm{mm}$, a square brick measuring $8\,\mathrm{mm}$ in thickness, as well as commercially available stone papers (Fig. 1a). The stone papers serve as eco-friendly alternatives to plastics and traditional papers as they are produced with less water, no wood, and hazardous materials. They are composed of limestone (calcium carbonate) and a thermoplastic resin. In this study, two variants of stone paper were used; $0.165\,\mathrm{mm}$ thick Limex having Polypropylene(PP) resin [37], as well as another stone paper with a thickness of $0.186\,\mathrm{mm}$, having high-density polyethylene (HDPE) resin [38].

A. Substrate properties

The atomic force microscopy (AFM) analysis reveals the surface roughness and morphology of the Limex paper, depicted as an inset in Fig. 1a. AFM measurements of brick, marble, and stone paper substrates were not possible due to their excessive roughness. The maximum height of the roughness and the root mean square (RMS) values of the Limex substrate are $77\,\mathrm{nm}$ and $4.6\,\mathrm{nm}$. Figs. 1b and 1c show

images of processed substrates and illustrate their different colors and appearances. Finally, to compare the compatibility of the different substrates with vacuum deposition tools, the outgassing time to reach a pressure of $2 \times 10^{-6}\,\mathrm{mbar}$, in the used sputter tool load lock, is shown in Fig. 1d. It is noteworthy that the outgassing duration for all substrates did not exceed $15\,\mathrm{min}$, indicating a manageable level of compatibility.

B. Device fabrication

Prior to fabrication, the selected substrates were cleaned using Isopropyl Alcohol (IPA) followed by air drying. Fabrication of the sensors is divided into two steps. First, thermistors were patterned by a $100\,\mathrm{nm}$ thin film of Copper (Cu) deposition onto the metal contacts pattern of a shadow mask. Having good electrical and thermal conductivity, cu facilitates efficient charge and heat transfer in the sensor. Cu deposition was done using a sputtering tool (Kenosistec, Italy) with a DC power of $150\,\mathrm{W}$ and a pure argon (Ar) atmosphere. Furthermore, to connect the two separated metal contacts of the sensor structures, $30\,\mathrm{nm}$ amorphous InGaZnO (IGZO) was sputtered over the entire structure of the sensor pattern utilizing an RF power of $75\,\mathrm{W}$, with IGZO serving as an n-type high electron mobility temperature-sensitive semiconductor. As an optimized thickness of IGZO was searched, first, $30\,\mathrm{nm}$ IGZO was deposited. However, the Limex stopped working after 3 weeks. Hence, $50\,\mathrm{nm}$ IGZO was sputtered to fabricate thermistors on the Limex. Fig. 1b shows fabricated thermistors on Marble, brick, stone paper, and Limex. The width of the Cu metal contacts and IGZO in between the Cu contacts are $583\,\mu\mathrm{m}$ and $764\,\mu\mathrm{m}$, respectively, Fig. 1c. Second, to fabricate the RTDs, $380\,\mathrm{nm}$ thin film of the biocompatible Zn metal was deposited onto the shadow mask patterns using a DC sputtering tool (see Fig. 5a).

C. Device Characterization

To characterize the electrical performance of the developed devices, on the one hand, the thermistors were placed on top of a hotplate, with sensor surface temperature monitored via a thermal camera. The signal acquisition was performed using an Arduino Uno R3 prototyping electronic board employing the voltage divider rule to obtain the resistance of the device at standard environmental conditions. The electrical analyses were performed by varying the temperature from $25\,^{\circ}\mathrm{C}$ to $80\,^{\circ}\mathrm{C}$. On the other hand, the RTDs characterization was carried out using a custom-made setup consisting of a chamber where the samples are placed and a dedicated data acquisition system, including a high-performance digital multimeter (Keithley Model 2000 with a 6 1/2-digit), a measuring unit (Keithley Series 2600B), and a developed LabView program. To set and vary the temperature serpentine heater was used. For the fabrication of the latter, commercial Ag paste (EC-1010 from LOCTITE) was screen-printed on Polyimide (Kapton) using a semi-automatic screen printer (C290, from Aurel automation S.P.A.) and consequently cured at $120\,^{\circ}\mathrm{C}$ for $15\,\mathrm{min}$. The heater was placed on top of the samples and a calibrated commercial PT100 sensor was used to measure the temperature (Fig. 5b).

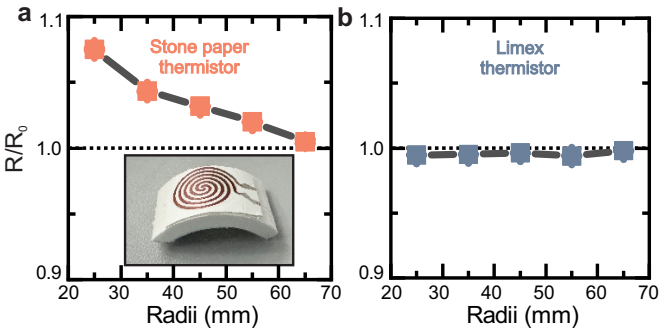

Fig. 4. Bending test of (a) stone paper thermistor and (b) Limex thermistor.

III. Results and Discussion

The electrical characterization of all sensors is performed using the described heating methodologies. Moreover, the light sensitivity of IGZO-based thermistors, and mechanical bending analyses of the two flexible thermistors were characterized. Furthermore, Zn-based RTDs dissolution tests were analyzed.

A. Thermistors sensing performance

The current-voltage characteristics of the thermistors are shown in Fig. 2a. Using linear ohmic behavior, the average resistances of thermistors fabricated on marble, brick, stone paper, and Limex substrates were determined to be $63\,\mathrm{k\Omega}$, $125\,\mathrm{k\Omega}$, $400\,\mathrm{k\Omega}$, and $1\,\mathrm{k\Omega}$, respectively, at room temperature. These values are comparable to those published previously for thin-film thermistors fabricated on Si, polyimide, glass, and polished alumina substrates [17], [40], [41]. Resistance variations of the thermistors in response to temperature changes while heating and cooling from $25\,^{\circ}\mathrm{C}$ to $80\,^{\circ}\mathrm{C}$ were observed through five cycles. The thermistors were deliberately limited in this temperature range to preserve the polymeric characteristics of stone paper and Limex substrates. This temperature range is important for human interaction, the design of electronic instruments, and integrated circuits [42]. The marble and brick thermistors have a small hysteresis from $45\,^{\circ}\mathrm{C}$ to $50\,^{\circ}\mathrm{C}$, as shown in Fig. 2b. However the two flexible thermistors show higher hysteresis from $40\,^{\circ}\mathrm{C}$ to $55\,^{\circ}\mathrm{C}$ and $45\,^{\circ}\mathrm{C}$ to $60\,^{\circ}\mathrm{C}$ for stone paper and Limex thermistors, respectively. The approximate linear sensitivity of the thermistors is $-11.54\,\%\,^{\circ}\mathrm{C}^{-1}$, $-7.98\,\%\,^{\circ}\mathrm{C}^{-1}$, $-7.49\,\%\,^{\circ}\mathrm{C}^{-1}$, and $-1.50\,\%\,^{\circ}\mathrm{C}^{-1}$ for heating and $-7.54\,\%\,^{\circ}\mathrm{C}^{-1}$, $-7.92\,\%\,^{\circ}\mathrm{C}^{-1}$, $-7.30\,\%\,^{\circ}\mathrm{C}^{-1}$, and $-5.16\,\%\,^{\circ}\mathrm{C}^{-1}$ for cooling for marble, brick, paper stone, and Limex thermistors, respectively. The marble thermistor has the highest absolute value of sensitivity among the four thermistors, whereas the Limex thermistor has the lowest. Compared to commercially available ceramic thermistors' sensitivity, which is between $-2\,\%\,^{\circ}\mathrm{C}^{-1}$ to $-6\,\%\,^{\circ}\mathrm{C}^{-1}$, the marble thermistor has an even greater sensitivity due to high thermal conductivity [43].

B. Thermistors reliability, light sensitivity, and bending deformation analyses

Fig. 3a presents the cycling plots for the thermistors. The cycling was performed with low heating and cooling rates to

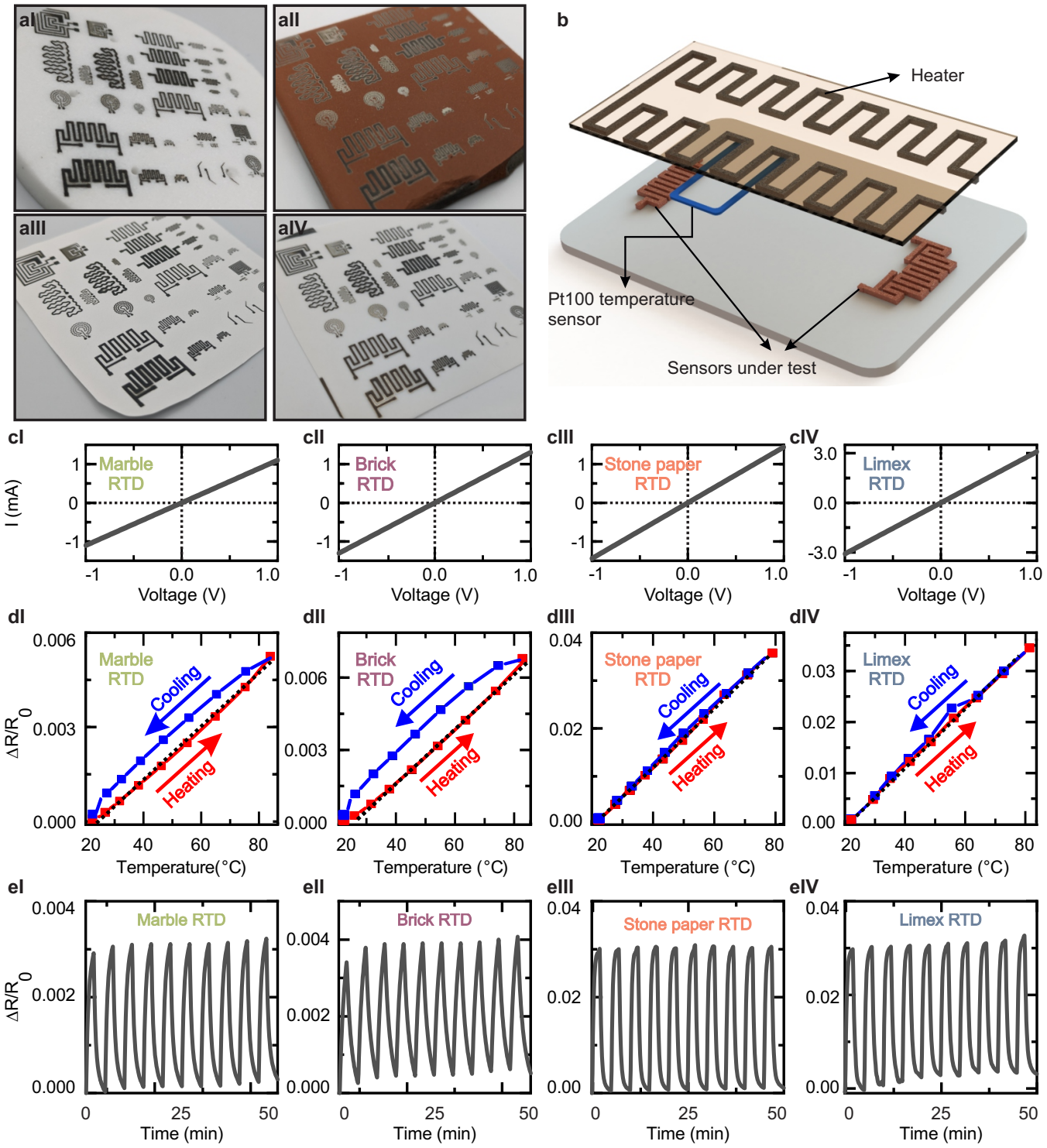

Fig. 5. RTDs structure, heating methodology, and performance: aI) Marble RTD, aII) brick RTD, aIII) stone paper RTD, and aIV) Limex RTD. b) Concept of heating methodology to the RTDs from above. c) Current-voltage characteristics of (cI) marble RTD, cII) brick RTD, cIII) stone paper RTD, and (cIV) Limex RTD. d) Calibration and normalized resistance versus temperature of (dI) marble RTD, dII) brick RTD, dIII) stone paper RTD, and (dIV) Limex RTD. e) Repeatability and sensitivity of (dI) marble RTD, dII) brick RTD, dIII) stone paper RTD, and (dIV) Limex RTD.

ensure the thermal equilibrium of the dense stone substrates with their environment. The thermistors showed stable signals after multiple cyclings. The average values of resistance at 25 °C (80 °C) are 120 kΩ (62 kΩ), 372 kΩ (197 kΩ) 256 kΩ (146 kΩ), and 2 kΩ (1 kΩ) for the marble, brick, stone paper, and Limex thermistors, respectively. The difference in extracted resistance at room temperature from the I-V curve is due to the measurement noise and the light sensitivity of IGZO material [21], [44]. Moreover, based on the fact that IGZO is a transparent and light-sensitive semiconductor, we analyzed the light sensitivity of the current-voltage characteristic of the thermistors, as shown in Fig. 3b. Results indicate that the

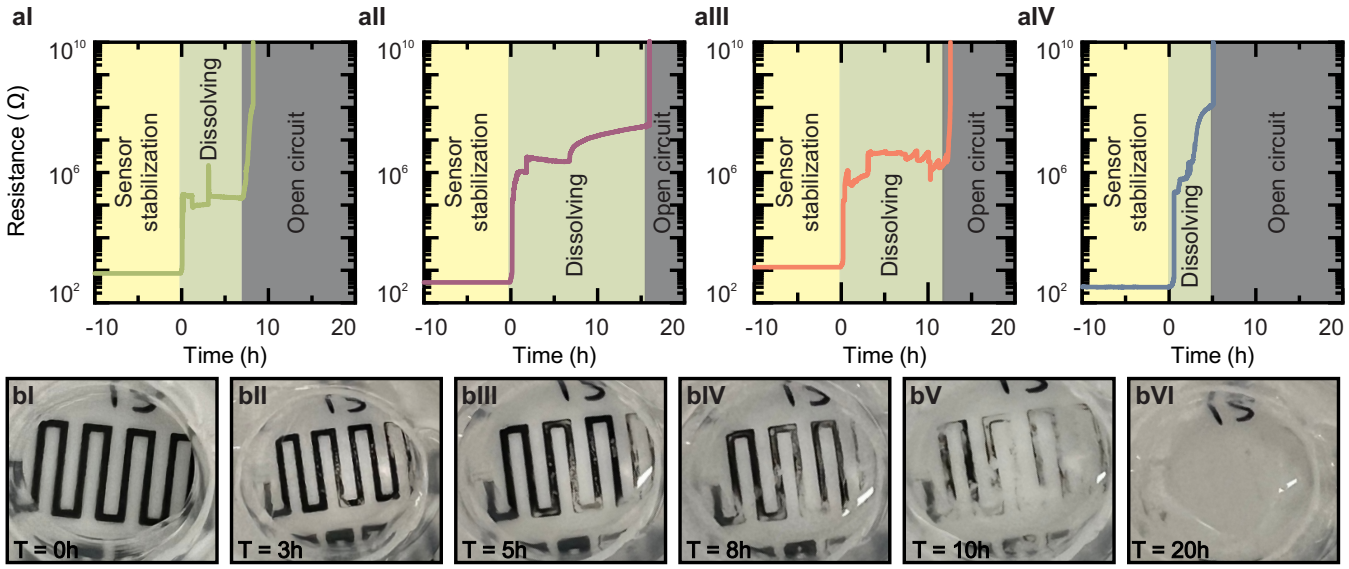

Fig. 6. Dissolution test: a) Dissolution profile of (aI) marble RTD, aII) brick RTD, aIII) stone paper RTD, and (aIV) Limex RTD after 10h stabilization time. b) Limex RTD dissolution test at (bI) T= 0h, bII) T= 3h, bIII) T= 5h, bIV) T= 8h, bV) T= 10h, and (bVI) T= 20h.

thermistors decreased their resistance in response to the light intensity. Furthermore, the mechanical properties of the two flexible sensors were characterized by bending the sensors at $65\,\mathrm{mm}$, $55\,\mathrm{mm}$, $45\,\mathrm{mm}$, $35\,\mathrm{mm}$, and $25\,\mathrm{mm}$, shown in Fig. 4. The stone paper thermistor showed a slight increase in resistance when bent to smaller radii (Fig. 4a), however, the average resistance of the Limex thermistor remained virtually unchanged and stopped working at the highest strain of about $0.37\,\%$ (Fig. 4b). Though IGZO shows decreased resistance under tensile strain [45], the stone paper thermistor showed a slight increase in resistance when bent to smaller radii due to the formation of microcracks and increased contact resistance in the overlapped region of IGZO and Cu thin films (Fig. 3a) [46]. This difference has roots in the different binding agent used in their composition. Limex is less likely to change electrical performance due to PP's good flexibility and fatigue resistance. However, stone paper is less likely to develop cracks when bent due to HDPE's excellent resistance to stress cracking [47].

C. RTDs sensing performance and reliability

The Zn-based RTDs are shown in Fig. 5a. A schematic of the heating methodology is shown in Fig. 5b. A heater was directly located on top of the sensors, and the temperature was monitored with a PT100 commercial temperature sensor. The current-voltage characteristics of the RTDs, shown in Fig. 5c, represent the ohmic contacts of the sensors with an average resistance of $906\,\Omega$, $765\,\Omega$, $693\,\Omega$, and $324\,\Omega$ extracted for marble, brick, stone paper, and Limex RTDs, respectively, at room temperature. The temperature sensitivity and hysteresis, shown at Figs. 5d were analyzed while the RTDs were exposed to temperature variation through ramping up and down between the temperatures of $25\,^{\circ}\mathrm{C}$ and $80\,^{\circ}\mathrm{C}$. The RTDs respond linearly to temperature variations. The temperature coefficient of resistance derived from the linear heating profile of marble, brick, stone paper, and Limex RTDs are $0.07\,^{\circ}\mathrm{C}^{-1}$, $0.05\,^{\circ}\mathrm{C}^{-1}$, $0.77\,^{\circ}\mathrm{C}^{-1}$, and $0.17\,^{\circ}\mathrm{C}^{-1}$, respectively. The temperature coefficient of resistance of our stone-based substrates is higher than that of $0.03\,^{\circ}\mathrm{C}^{-1}$ for $200\,\mathrm{nm}$ thermal evaporated Zn on a glass substrate. This is due to the higher Zn deposition thickness. Because the temperature coefficient of resistivity increases as the film thickness increases [48]. Stone paper and Limex RTDs show minimal differences in resistance during heating and cooling cycles as compared to marble and brick RTDs, which have a larger hysteresis. This is in contrast to the analysis for the thermistor hysteresis shown in Section II-A. This could be because of the difference in sensor material, stabilization time, and heating methodologies. Adjusting the material thickness, refining fabrication techniques, and encapsulating the sensors can improve sensors performance The reliability of the RTDs signals was tested through 10 cycles shown in Fig. 5d. All the stone-based RTDs show quite stable responses for multiple cycling within the range of $25\,^{\circ}\mathrm{C}$ and $80\,^{\circ}\mathrm{C}$.

D. RTDs dissolution rate

Fig. 6a shows the dissolution rate of the sputtered Zn on the stone-based substrates. The electrical resistances of the samples were observed continuously for approximately $10\,\mathrm{h}$ in the absence of water. Subsequently, $800\,\mu\mathrm{L}$ of deionized (DI) water was added to each sample. Following this addition, a rapid increase in resistance was observed, reaching the Megaohm range. This can be attributed to the resistance of DI water. The high surface roughness of brick compared to the marble caused absorption of DI water thus taking a longer time for the resistance to approach infinity. Moreover, the higher water absorption rate of the PP resin in the Limex substrate resulted in faster dissolution compared to stone paper [47]. The entire Zn sputtered on all the substrates dissolved in less than 36 hours. Encapsulating the sensors can help maintain consistent electrical performance during the initial stages of

dissolution. However, our primary objective here is to demonstrate the complete biodegradability of the sensors. Fig. 6b shows the dissolution rate of Limex RTD at 0h, 3h, 5h, 8h, 10h, and 20h. These results highlight a significant step forward in making green and innovative electronic components, offering sustainable solutions that help protect the environment using eco-friendly and advanced technologies.

IV. Conclusion

The study shows that using vacuum deposition techniques enables thin-film thermistors and RTDs to be placed on unconventional, eco-friendly stone-based substrates such as marble, brick, stone paper, and Limex. The sensors' performance was evaluated across the 25 °C to 80 °C temperature range using both a hotplate and a localized heating method. The marble thermistors showed superior sensitivity, while stone paper and Limex RTDs exhibited minimal hysteresis. In addition, the IGZO-based thermistors are light-sensitive. The flexible stone paper thermistors are sensitive to bending and their resistance increases with a decrease in bending radius. Moreover, Zn-based RTDs can be dissolved in less than two days. Our results show that temperature sensors on such unconventional surfaces which are environmentally sustainable alternatives can combine good sensing performance, and repeatability with the environmental friendliness, availability, and aesthetics of natural stone.

References

[1] P. Wang, M. Hu, H. Wang, Z. Chen, Y. Feng, J. Wang, W. Ling, and Y. Huang, "The evolution of flexible electronics: from nature, beyond nature, and to nature," *Advanced Science*, vol. 7, no. 20, p. 2001116, 2020. [Online]. Available: https://doi.org/10.1002/advs.202001116

[2] B. Saha, S. Baek, and J. Lee, "Highly sensitive bendable and foldable paper sensors based on reduced graphene oxide," *ACS applied materials & interfaces*, vol. 9, no. 5, pp. 4658–4666, 2017. [Online]. Available: https://doi.org/10.1021/acsami.6b10484

[3] N. S. Khaanghah, H. de Souza Oliveira, R. Riaz, F. Catania, M. A. C. Angeli, L. Petti, G. Cantarella, and N. Münzenrieder, "Silicone/carbon black-filled elastomer based self-healing strain sensor," *IEEE Sensors Letters*, 2023. [Online]. Available: https://doi.org/10.1109/LSENS.2023.3273618

[4] T. Someya, Y. Kato, T. Sekitani, S. Iba, Y. Noguchi, Y. Murase, H. Kawaguchi, and T. Sakurai, "Conformable, flexible, large-area networks of pressure and thermal sensors with organic transistor active matrixes," *Proceedings of the National Academy of Sciences*, vol. 102, no. 35, pp. 12 321–12 325, 2005. [Online]. Available: https://doi.org/10.1073/pnas.0502392102

[5] J. C. Costa, F. Spina, P. Lugoda, L. Garcia-Garcia, D. Roggen, and N. Münzenrieder, "Flexible sensors—from materials to applications," *Technologies*, vol. 7, no. 2, p. 35, 2019. [Online]. Available: https://doi.org/10.3390/technologies7020035

[6] S. Mlakar, M. Alida Haberfellner, H.-C. Jetter, and M. Haller, "Exploring affordances of surface gestures on textile user interfaces," in *Designing Interactive Systems Conference 2021*, ser. DIS '21. New York, NY, USA: Association for Computing Machinery, 2021, p. 1159–1170. [Online]. Available: https://doi.org/10.1145/3461778.3462139

[7] A. Nag, S. C. Mukhopadhyay, and J. Kosel, "Wearable flexible sensors: A review," *IEEE Sensors Journal*, vol. 17, no. 13, pp. 3949–3960, 2017. [Online]. Available: https://doi.org/10.1109/JSEN.2017.2705700

[8] M. Cheng, G. Zhu, F. Zhang, W.-l. Tang, S. Jianping, J.-q. Yang, and L.-y. Zhu, "A review of flexible force sensors for human health monitoring," *J. Adv. Res.*, vol. 26, pp. 53–68, Nov. 2020. [Online]. Available: https://doi.org/10.1016/j.jare.2020.07.001

[9] X.-H. Zhao, S.-N. Ma, H. Long, H. Yuan, C. Y. Tang, P. K. Cheng, and Y. H. Tsang, "Multifunctional sensor based on porous carbon derived from metal–organic frameworks for real time health monitoring," *ACS Applied Materials & Interfaces*, vol. 10, no. 4, pp. 3986–3993, 2018, pMID: 29303248. [Online]. Available: https://doi.org/10.1021/acsami.7b16859

[10] S. Nakata, T. Arie, S. Akita, and K. Takei, "Wearable, flexible, and multifunctional healthcare device with an isfet chemical sensor for simultaneous sweat ph and skin temperature monitoring," *ACS sensors*, vol. 2, no. 3, pp. 443–448, 2017. [Online]. Available: https://doi.org/10.1021/acssensors.7b00047

[11] F. Zhang, Y. Zang, D. Huang, C.-a. Di, and D. Zhu, "Flexible and self-powered temperature–pressure dual-parameter sensors using microstructure-frame-supported organic thermoelectric materials," *Nature communications*, vol. 6, no. 1, p. 8356, 2015. [Online]. Available: https://doi.org/10.1038/ncomms9356

[12] L. Wang, R. Zhu, and G. Li, "Temperature and strain compensation for flexible sensors based on thermosensation," *ACS applied materials & interfaces*, vol. 12, no. 1, pp. 1953–1961, 2019. [Online]. Available: https://doi.org/10.1021/acsami.9b21474

[13] T. Q. Trung, S. Ramasundaram, B.-U. Hwang, and N.-E. Lee, "An all-elastomeric transparent and stretchable temperature sensor for body-attachable wearable electronics," *Advanced materials*, vol. 28, no. 3, pp. 502–509, 2016. [Online]. Available: ttps://doi.org/10.1002/adma.201504441

[14] B. Davaji, H. D. Cho, M. Malakoutian, J.-K. Lee, G. Panin, T. W. Kang, and C. H. Lee, "A patterned single layer graphene resistance temperature sensor," *Scientific reports*, vol. 7, no. 1, p. 8811, 2017. [Online]. Available: https://doi.org/10.1038/s41598-017-08967-y

[15] H. de Souza Oliveira, F. Catania, G. Cantarella, V. Benedetti, M. Baratieri, and N. Münzenrieder, "Recycled carbon-based strain sensors: An ecofriendly approach using char and coconut oil," in *2021 IEEE International Flexible Electronics Technology Conference (IFETC)*. IEEE, 2021, pp. 0053–0055. [Online]. Available: https://doi.org/10.1109/IFETC49530.2021.9580526

[16] G. Cantarella, M. Madagalam, I. Merino, C. Ebner, M. Ciocca, A. Polo, P. Ibba, P. Bettotti, A. Mukhtar, B. Shkodra, A. S. Inam, A. J. Johnson, A. Pouryazdan, M. Paganini, R. Tiziani, T. Mimmo, S. Cesco, N. Münzenrieder, L. Petti, N. Cohen, and P. Lugli, "Laser-induced, green and biocompatible paper-based devices for circular electronics (adv. funct. mater. 17/2023)," *Advanced Functional Materials*, vol. 33, no. 17, p. 2370106, 2023. [Online]. Available: https://onlinelibrary.wiley.com/doi/abs/10.1002/adfm.202370106

[17] H. D. S. Oliveira, F. Catania, A. H. Lanthaler, A. Carrasco-Pena, G. Cantarella, and N. Münzenrieder, "Substrate-free transfer of large-area ultra-thin electronics," *Advanced Electronic Materials*, vol. n/a, no. n/a, p. 2201281. [Online]. Available: https://onlinelibrary.wiley.com/doi/abs/10.1002/aelm.202201281

[18] Y. Guo, S. Chen, L. Sun, L. Yang, L. Zhang, J. Lou, and Z. You, "Degradable and fully recyclable dynamic thermoset elastomer for 3d-printed wearable electronics," *Advanced Functional Materials*, vol. 31, no. 9, p. 2009799, 2021. [Online]. Available: https://doi.org/10.1002/adfm.202009799

[19] M. J. Tan, C. Owh, P. L. Chee, A. K. K. Kyaw, D. Kai, and X. J. Loh, "Biodegradable electronics: cornerstone for sustainable electronics and transient applications," *Journal of Materials Chemistry C*, vol. 4, no. 24, pp. 5531–5558, 2016. [Online]. Available: https://doi.org/10.1039/C6TC00678G

[20] H. de Souza Oliveira, A. Nijkoops, M. Ciocca, A. Carrasco-Peña, L. Petti, G. Cantarella, and N. Münzerieder, "Flexible Auxetic Structure as Substrates for Resistive Pressure Sensors," in *2022 IEEE Sensors*. IEEE, Oct. 2022, pp. 01–04. [Online]. Available: https://doi.org/10.1109/SENSORS52175.2022.9967254

[21] H. de Souza Oliveira, N. S. Khaanghah, V. Y. Han, A. Carrasco-Pena, A. Ion, M. Haller, G. Cantarella, and N. Münzenrieder, "Permeable thermistor temperature sensors based on porous melamine foam," *IEEE Sensors Letters*, vol. 7, no. 5, pp. 1–4, 2023. [Online]. Available: https://doi.org/10.1109/LSENS.2023.3271590

[22] N. Münzenrieder, G. Cantarella, C. Vogt, L. Petti, L. Büthe, G. A. Salvatore, Y. Fang, R. Andri, Y. Lam, R. Libanori, D. Widner, A. R. Studart, and G. Tröster, "Stretchable and conformable oxide thin-film electronics," *Advanced Electronic Materials*, vol. 1, no. 3, p. 1400038, 2015. [Online]. Available: https://onlinelibrary.wiley.com/doi/abs/10.1002/aelm.201400038

[23] N. Lovecchio, V. Di Meo, D. Caputo, A. Nascetti, A. Crescitelli, E. Esposito, and G. de Cesare, "Transparent oxide/metal/oxide thin film heater with integrated resistive temperature sensors," *IEEE Sensors*

Journal, vol. 21, no. 17, pp. 18 847–18 854, 2021. [Online]. Available: https://doi.org/10.1109/JSEN.2021.3090030

[24] M. Ahmed, M. M. Chitteboyina, D. P. Butler, and Z. Celik-Butler, "Temperature sensor in a flexible substrate," *IEEE Sensors Journal*, vol. 12, no. 5, pp. 864–869, 2011. [Online]. Available: https://doi.org/10.1109/JSEN.2011.2166064

[25] F. Catania, H. de Souza Oliveira, P. Lugoda, G. Cantarella, and N. Münzenrieder, "Thin-film electronics on active substrates: review of materials, technologies and applications," *Journal of Physics D: Applied Physics*, vol. 55, no. 32, p. 323002, may 2022. [Online]. Available: https://dx.doi.org/10.1088/1361-6463/ac6af4

[26] F. Brunetti, A. Operamolla, S. Castro-Hermosa, G. Lucarelli, V. Manca, G. M. Farinola, and T. M. Brown, "Printed solar cells and energy storage devices on paper substrates," *Advanced Functional Materials*, vol. 29, no. 21, p. 1806798, 2019. [Online]. Available: https://doi.org/10.1002/adfm.201806798

[27] D.-Y. Yoon and D.-G. Moon, "Bright flexible organic light-emitting devices on copy paper substrates," *Current Applied Physics*, vol. 12, pp. e29–e32, 2012. [Online]. Available: https://doi.org/10.1016/j.cap.2011.04.033

[28] M. Landers and S. Choi, "Small-scale, storable paper biobatteries activated via human bodily fluids," *Nano Energy*, vol. 97, p. 107227, 2022. [Online]. Available: ttps://doi.org/10.1016/j.nanoen.2022.107227

[29] Y. Xu, Q. Fei, M. Page, G. Zhao, Y. Ling, S. B. Stoll, and Z. Yan, "based wearable electronics," *Iscience*, vol. 24, no. 7, 2021. [Online]. Available: https://doi.org/10.1016/j.isci.2021.102736

[30] R. Martins, D. Gaspar, M. J. Mendes, L. Pereira, J. Martins, P. Bahubalindruni, P. Barquinha, and E. Fortunato, "Papertronics: Multigate paper transistor for multifunction applications," *Applied Materials Today*, vol. 12, pp. 402–414, 2018. [Online]. Available: https://doi.org/10.1016/j.apmt.2018.07.002

[31] J. Shah and R. Malcolm Brown, "Towards electronic paper displays made from microbial cellulose," *Applied microbiology and biotechnology*, vol. 66, pp. 352–355, 2005. [Online]. Available: https://doi.org/10.1007/s00253-004-1756-6

[32] L. Yang, A. Rida, R. Vyas, and M. M. Tentzeris, "Rfid tag and rf structures on a paper substrate using inkjet-printing technology," *IEEE transactions on microwave theory and techniques*, vol. 55, no. 12, pp. 2894–2901, 2007. [Online]. Available: https://doi.org/10.1109/TMTT.2007.909886

[33] C. Chu and P. Nel, "Characterisation and deterioration of mineral papers," *AICCM Bulletin*, vol. 40, no. 1, pp. 37–49, 2019. [Online]. Available: https://doi.org/10.1080/10344233.2019.1672951

[34] C. Varodi, F. Pogacean, M. Gheorghe, V. Mirel, M. Coros, L. Barbu-Tudoran, R.-I. Stefan-van Staden, and S. Pruneanu, "Stone paper as a new substrate to fabricate flexible screen-printed electrodes for the electrochemical detection of dopamine," *Sensors*, vol. 20, no. 12, p. 3609, 2020. [Online]. Available: https://doi.org/10.3390/s20123609

[35] J. He, M. Luo, L. Hu, Y. Zhou, S. Jiang, H. Song, R. Ye, J. Chen, L. Gao, and J. Tang, "Flexible lead sulfide colloidal quantum dot photodetector using pencil graphite electrodes on paper substrates," *Journal of Alloys and Compounds*, vol. 596, pp. 73–78, 2014. [Online]. Available: https://doi.org/10.1016/j.jallcom.2014.01.194

[36] N. S. Khaanghah, H. de Souza Oliveira, A. Carrasco-Pena, G. Cantarella, M. Haller, N. Rapagnani, A. van Bezooijen, M. Nippa, and N. Münzenrieder, "Stone-based substrates for thin-film thermistor temperature sensors," in *2023 IEEE SENSORS*. IEEE, 2023, pp. 01–04. [Online]. Available: https://doi.org/10.1109/SENSORS56945.2023.10325074

[37] Times Bridge Management Company, LTD., "LIMEX," Retrieved from https://tb-m.com/en/products/products-limex/.

[38] Taiwan Lung Meng Technology Company, LTD., "Stone Paper," Retrieved from https://stone-paper.nl/home.

[39] M. Irimia-Vladu, ""green" electronics: biodegradable and biocompatible materials and devices for sustainable future," *Chemical Society Reviews*, vol. 43, no. 2, pp. 588–610, 2014. [Online]. Available: https://doi.org/10.1039/C3CS60235D

[40] G. Urban, A. Jachimowicz, F. Kohl, H. Kuttner, F. Olcaytug, H. Kamper, F. Pittner, E. Mann-Buxbaum, T. Schalkhammer, O. Prohaska *et al.*, "High-resolution thin-film temperature sensor arrays for medical applications," *Sensors and Actuators A: Physical*, vol. 22, no. 1-3, pp. 650–654, 1990. [Online]. Available: https://doi.org/10.1016/0924-4247(89)80051-2

[41] I. W. Kwon, H. J. Son, W. Y. Kim, Y. S. Lee, and H. C. Lee, "Thermistor behavior of pedot: Pss thin film," *Synthetic metals*, vol. 159, no. 12, pp. 1174–1177, 2009. [Online]. Available: https://doi.org/10.1016/j.synthmet.2009.02.006

[42] H. Al-Mumen, F. Rao, L. Dong, and W. Li, "Design, fabrication, and characterization of graphene thermistor," in *The 8th Annual IEEE International Conference on Nano/Micro Engineered and Molecular Systems*. IEEE, 2013, pp. 1135–1138. [Online]. Available: https://doi.org/10.1109/NEMS.2013.6559922

[43] A. Feteira, "Negative temperature coefficient resistance (ntcr) ceramic thermistors: an industrial perspective," *Journal of the American Ceramic Society*, vol. 92, no. 5, pp. 967–983, 2009. [Online]. Available: https://doi.org/10.1111/j.1551-2916.2009.02990.x

[44] J. Yao, N. Xu, S. Deng, J. Chen, J. She, H.-P. D. Shieh, P.-T. Liu, and Y.-P. Huang, "Electrical and photosensitive characteristics of a-igzo tfts related to oxygen vacancy," *IEEE Transactions on Electron Devices*, vol. 58, no. 4, pp. 1121–1126, 2011. [Online]. Available: https://doi.org/10.1109/TED.2011.2105879

[45] Q. Zheng, J.-h. Lee, X. Shen, X. Chen, and J.-K. Kim, "Graphene-based wearable piezoresistive physical sensors," *Materials Today*, vol. 36, pp. 158–179, 2020. [Online]. Available: https://doi.org/10.1016/j.mattod.2019.12.004

[46] B. Wang, A. Thukral, Z. Xie, L. Liu, X. Zhang, W. Huang, X. Yu, C. Yu, T. J. Marks, and A. Facchetti, "Flexible and stretchable metal oxide nanofiber networks for multimodal and monolithically integrated wearable electronics," *Nature communications*, vol. 11, no. 1, p. 2405, 2020. [Online]. Available: https://doi.org/10.1038/s41467-020-16268-8

[47] A. H. Awad, R. El Gamasy, A. Abd El Wahab, and M. H. Abdellatif, "Mechanical and physical properties of pp and hdpe," *Eng. Sci*, vol. 4, no. 2, p. 34, 2019.

[48] M. E. Shabasy, M. E. Hiti, and M. Ahmed, "Electrical properties of thin metal zinc films," *Journal of materials science*, vol. 25, pp. 585–588, 1990. [Online]. Available: https://doi.org/10.1007/BF00714079